

Mirror nuclei emission and isospin transport at intermediate energies

I.Lombardo^{a,c}, C.Agodi^a, R.Alba^a, F.Amorini^{a,c}, A.Anzalone^a, I.Berceanuⁱ, M.B.Chatterjee^d, G.Cardella^b, S.Cavallaro^{a,c}, R.Coniglione^a, E.De Filippo^b, A.Di Pietro^a, P.Figuera^a, E.Geraci^{b,c}, G.Giuliani^c, L.Grassi^{b,c}, A.Grzeszczuk^h, E.La Guidara^{b,e}, G.Lanzalone^{a,f}, N.Le Neindre^g, C.Maiolino^a, A.Pagano^b, M.Papa^b, S.Pirrone^b, A.Popⁱ, G.Politi^{b,c}, F.Porto^{a,c}, F.Rizzo^{a,c}, P.Russotto^{a,c}, D.Santonocito^a, P.Sapienza^a and G.Verde^b

- a) INFN, Laboratori Nazionali del Sud, Catania, Italy
- b) INFN, Sezione di Catania, Catania, Italy
- c) Dipartimento di Fisica e Astronomia, Università di Catania, Catania, Italy
- d) Saha Institute of Nuclear Physics, Kolkata, India
- e) CSFNSM, Catania, Italy
- f) Università Kore di Enna, Enna, Italy
- g) Institut de Physique Nucleaire d'Orsay, CNRS-IN2P3, Orsay Cedex, France
- h) Institute of Physics, University of Silesia, Katowice, Poland
- i) Institute for Physics and Nuclear Engineering, Bucharest, Romania

Abstract

Isospin effects are studied in reactions induced by ^{40}Ca projectiles at $E/A=25$ MeV on ^{40}Ca , ^{48}Ca and ^{46}Ti targets. The N/Z of projectile-like, target-like and mid-velocity sources are probed by measuring isotopic ($^7\text{Li}/^6\text{Li}$ and $^9\text{Be}/^7\text{Be}$) and isobaric ($^7\text{Li}/^7\text{Be}$) yield ratios, for semi-peripheral events. The presence of isospin diffusion and drift phenomena is observed. It seems indeed that the interaction time between projectile and target does not allow a complete charge equilibration between quasi-projectile and quasi-target sources.

1 Introduction

In the last decade studies on isotopic effects involved in reaction mechanisms and in fragment production have become increasingly important [1-7]. Through the overlap region produced in the early stages of a semi-peripheral reaction between the interacting projectile and target systems, *isospin transport* phenomena can occur [2]. In more detail, isospin transport phenomena have essentially two facets: *isospin diffusion* and *isospin drift*. Isospin diffusion is related to the differences in N/Z of interacting projectile and target nuclei; the minimization of the free-energy during the interaction time tends to equilibrate the N/Z content of the whole di-nuclear system. If the interaction time between projectile and target is long enough, as for the case of low bombarding energies ($E < 10 \text{ MeV/A}$), the nucleon exchange process leads to a uniform distribution of the N/Z asymmetry throughout the whole system [8]. Increasing the bombarding energies, the interaction time between the reaction partners is reduced and the N/Z degree of freedom does not have the time to uniformly distribute throughout the system [9,10]. These isotopic effects can be observed in the framework of microscopic models. For example, we have run calculations of mid-peripheral ($b=7 \text{ fm}$) $^{40}\text{Ca}+^{48}\text{Ca}$ collisions at $E/A=25$ MeV with CoMD-II and IBUU04 codes [11,12], and we have observed (Figure 1) that after the re-separation time between the QP and QT interacting partners ($\approx 150 \text{ fm/c}$), the N/Z values of QP and QT excited sources are different with $\Delta(N/Z) \approx 0.12$; therefore it seems that a complete charge equilibration along the di-nuclear system is not fully reached.

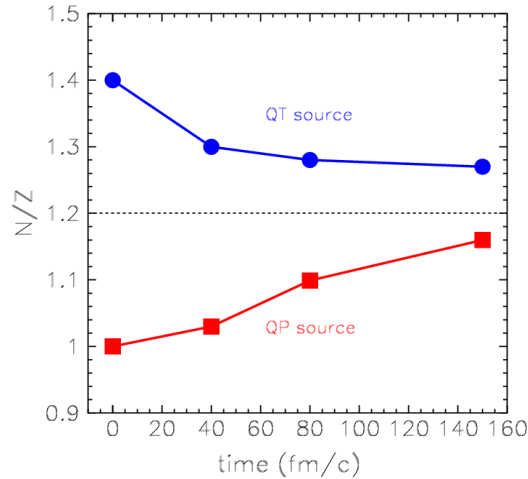


Fig. 1: IBUU04 calculation of N/Z evolution, for QP and QT sources, in $^{40}\text{Ca}+^{48}\text{Ca}$ collision at 25MeV/A and $b=7\text{fm}$.

The second facet of isospin transport phenomena is constituted by *isospin drift*. This effect is related to the gradient of nuclear density involving the overlap region between the interacting nuclei; in particular, stronger the gradient of density reached during the first phase of the collision, greater the neutron content of the emitted light fragments. This effect becomes noticeable only if the bombarding energies are relatively high, as in the case of intermediate energy collisions; in this case the gradient of density is stronger and the neutron enrichment of the matter belonging to the mid-velocity (MV) overlap region becomes clearly visible [13,14].

From a theoretical point of view, isospin diffusion and drift phenomena constitute one of the strongest ways to disentangle the poorly-known behaviour of the density related part of the iso-vectorial term in the nuclear Equation of State [6].

Experimentally, the N/Z values of the QP, QT and MV sources can be probed by measuring isotopic distributions of produced fragments [15,16] or by extracting the ratio between the yields of emitted isobar nuclei, i.e. $Y(^3\text{H})/Y(^3\text{He})$, $Y(^7\text{Li})/Y(^7\text{Be})$, and $Y(^{11}\text{B})/Y(^{11}\text{C})$. These latter approaches assume that isobar ratios reflect the initial neutron/proton composition (N/Z) of their emitting sources [16,17].

In this work we report on isospin transport phenomena by looking at the production of isotopes ($^6,7\text{Li}$ and $^7,9\text{Be}$) and isobars (^7Li and ^7Be) in $^{40}\text{Ca}+^{40,48}\text{Ca}$, ^{46}Ti collisions at $E/A=25$ MeV, by means of the CHIMERA detector, as described in Section 2. The yield ratios of n-rich to n-poor isotopes (i.e. $^7\text{Li}/^6\text{Li}$ and $^9\text{Be}/^7\text{Be}$) as a function of the parallel velocity are shown in Section 3. In Section 4 we study the isobaric emission by looking at the kinetic energy spectra of ^7Li and ^7Be . We perform a three component moving source analysis in order to obtain an estimate of the emission yields from QP, QT and MV sources. The data analysis shown in Sects. 3,4 seems to testify clearly the presence of isospin diffusion between projectile and target having large N/Z difference. It seems moreover that the complete charge equilibrium through the di-nuclear system has not been reached during the interaction time for semi-peripheral collisions. Finally, the analysis of fragments emitted at MV shows an abundant emission of n-rich clusters compared to n-poor ones, as expected in the presence of isospin drift effects.

2 Experimental apparatus

The experiment was performed at the INFN–LNS Superconducting Cyclotron facility in Catania (Italy). A beam of ^{40}Ca at 25 MeV/A having an intensity of about 200 ppA impinged on self–

supporting isotopically enriched targets of ^{40}Ca (1.24 mg/cm²), ^{48}Ca (2.87 mg/cm²) and ^{46}Ti (1.06 mg/cm²). Emitted fragments were detected by the CHIMERA 4 π array. Details about the CHIMERA array and its detection and identification capabilities are described in Refs. [18-20]. We analysed only events where the total detected charge was between 80% and 100% of the total charge, Z_{tot} , in the entrance channel of the reaction ($Z_{tot}=40$ and 42 for Ca and Ti targets, respectively). Quasi-elastic reactions were removed during the experiment by the chosen electronics trigger condition, requiring the detection of at least 3 charged particles with $Z>1$. This work focuses on the detection of different isotopes and isobars, as ^6Li , ^7Li and ^7Be , ^9Be identified by means of a ΔE - E energy loss technique in the Silicon-CsI(Tl) telescopes of CHIMERA. The resulting identification threshold is about 7 MeV/A. The kinetic energies of identified fragments are measured from the energy deposited in the silicon detectors, with an uncertainty $\delta E_{kin}/E_{kin}\approx 2\%$ for a single telescope. Unfortunately, due to technical problems, the beam time delivered for the realization of the whole experiment was relatively low (1 day). Due to the poor statistics, we perform our data analysis looking at inclusive events, taking into account that, for geometrical reasons, the bulk of events belonging to such a class is widely dominated by semi-peripheral collisions.

3 Isotopic emission

One of the first observables used since the beginning of nuclear isospin physics concerns the relative yields between the different isotopes emitted in a fragmentation event. It was observed in fact that the N/Z of entrance channel strongly influences the isotopic emission. In particular, greater is the N/Z ratio of the entrance channel, greater are the yields of neutron rich isotopes compared to the proton rich ones [21]. Such kind of observations indicate the strong role played by the N/Z degree of freedom during the fragmentation phase of the nuclear matter. A common way for investigating such isotopic effects consists in the observation of the ratio between the emission yields of a couple of isotopes (for example $^7\text{Li}/^6\text{Li}$ and $^9\text{Be}/^7\text{Be}$) as a function of their parallel velocity [22]. In such way, very particular aspects of heavy ion collisions at medium energies have been observed. For example, a considerable neutron enrichment of particles emitted at MV has been observed in different experiments, consistent with the theoretically predicted isospin drift phenomenon [2]. In order to have information on such thematic, we have plotted the yield ratios for the isotopes $^7\text{Li}/^6\text{Li}$ and $^9\text{Be}/^7\text{Be}$ as a function of the different bins of parallel velocity (Figure 2).

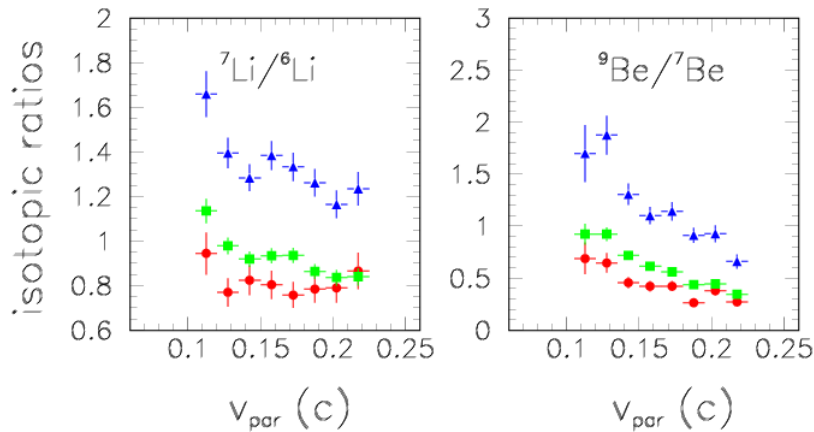


Fig. 2: Yield ratio for the emitted isotopes $^7\text{Li}/^6\text{Li}$ and $^9\text{Be}/^7\text{Be}$ as a function of the different bins of parallel velocity (in c units, in laboratory frame). Blue triangles: $^{40}\text{Ca}+^{48}\text{Ca}$ reaction. Green squares: $^{40}\text{Ca}+^{46}\text{Ti}$ reaction. Red circles: $^{40}\text{Ca}+^{40}\text{Ca}$ reaction.

We clearly observe that the MV emission (having v_{par} near $0.12c$) shows higher probability of emitting n-rich isotopes than n-poor ones, with respect to the region of parallel velocity near to the projectile velocity ($v_{\text{par}} \approx 0.2c$). This effect could be attributed, especially for the N/Z symmetric collision $^{40}\text{Ca}+^{40}\text{Ca}$, to the isospin drift process, leading to a neutron enrichment of clusters emitted at MV.

It is also interesting to observe that, even if the projectile beam used in all the reactions was the same (^{40}Ca , $N/Z=1$), the isotopic relative yields for the fragments emitted in the region of parallel velocity near to the projectile one ($v_{\text{par}} \approx 0.2c$) are noticeably different for the three reactions, and they seem to be directly related to the N/Z of the different targets; in particular we observe an enhancement of emission of neutron-rich isotopes for the reaction involving the target with a great isospin asymmetry (^{48}Ca ; $N/Z=1.4$) compared to the other targets (^{40}Ca and ^{46}Ti , having respectively $N/Z = 1$ and $N/Z = 1.09$). This effect is probably due to the fact that at these energies of 25 MeV/A it is possible, for semi-peripheral reactions, to observe isospin diffusion effects for the reaction involving projectile and target nuclei with high gradient in N/Z ($^{40}\text{Ca}+^{48}\text{Ca}$). In our case this phenomenon leads to an increase of the N/Z of the QP source, that we experimentally infer by observing the increased isotopic yield ratios.

The isotopic yield ratios have the advantage of being established between nuclei that experience the same Coulomb interaction when they are emitted by a given source, but also they have the disadvantage of involving isotopes, i.e. nuclei with different masses, that participate differently in the excitation energy sharing during the fragmentation events. In order to overcome such problems, and to have other information about the isotopic composition of the different sources emitting fragments in a nuclear reaction at intermediate energies, in the next paragraph we look at the yield ratios of the light mirror nuclei ^7Li and ^7Be emitted in the analysed reactions.

4 Mirror isobar nuclei emission

It has been shown by different collaborations [16,17] that a way for inferring information on the N/Z content of a given emitting source consists of looking at the yield ratios of pairs of light isobars, as $t/{}^3\text{He}$ or ${}^7\text{Li}/{}^7\text{Be}$. Figure 3 shows ${}^7\text{Li}$ and ${}^7\text{Be}$ kinetic energy spectra measured at polar angles $\theta=11.5^\circ, 14.5^\circ, 18^\circ, 22^\circ, 27^\circ, 34^\circ, 42^\circ, 50^\circ, 58^\circ, 66^\circ$ in the laboratory frame for the ${}^{40}\text{Ca}+{}^{46}\text{Ti}$ reaction.

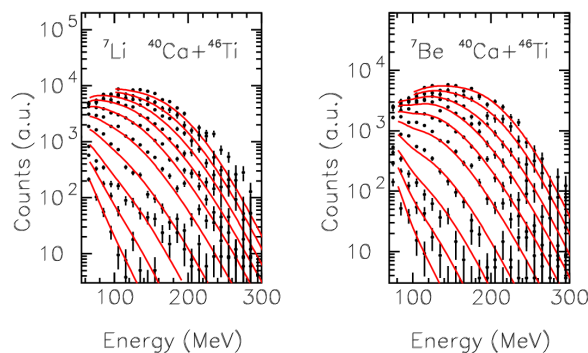


Fig. 3: Inclusive energy spectra for ${}^7\text{Li}$ and ${}^7\text{Be}$ emitted in the ${}^{40}\text{Ca}+{}^{46}\text{Ti}$ reaction, at different values of polar angle in the laboratory frame (respectively $11.5^\circ, 14.5^\circ, 18^\circ, 22^\circ, 27^\circ, 34^\circ, 42^\circ, 50^\circ, 58^\circ, 66^\circ$). The solid red line is the result of the three moving sources fits, described in the text.

We performed a multi component moving source analysis of these energy spectra [23-25]. In order to evaluate the contributions to the spectra due to QT emission (that is partially cut by the identification thresholds) we tried (as first step) to fit the spectra with only two moving sources, representing the QP

and MV source emission (whose emitted fragments are well detected because of the advantageous kinematics). The result is that the spectra of particles emitted at the higher polar angles ($\theta \geq 50^\circ$) are not well reproduced. Therefore, the data are well reproduced only by assuming that they originate from the superposition of three Maxwellian distributions of the form [23,24,25]:

$$\frac{d^2N}{dEd\Omega} = \sum_{i=1}^3 N_i (E - E_C)^{1/2} \exp \left[- \frac{E - E_C + E_{S,i} - 2(E - E_C)^{1/2} \sqrt{E_{S,i}} \cos \theta}{T_i} \right] \quad (1)$$

The Maxwellian distributions correspond to the emission from the QT ($i=1$), the MV ($i=2$) and the QP ($i=3$) source. The i^{th} source emits at temperature T_i and moves along the beam axis with a velocity v_{si} in the laboratory reference frame. In Eq. (1), $E_{S,i} = \frac{1}{2} m v_{si}^2$ is the kinetic energy of a particle moving with a velocity equal to the emitting source one. The normalization constants, N_i , the temperatures, T_i , the velocities of the sources, v_{si} , and the Coulomb barrier, E_C , are determined as free parameters from the best-fit to the experimental data. The solid red lines on Figure 3 show the results of the fitting procedure. The overall agreement with the measured energy spectra is satisfactory. The obtained fit parameters are in reasonable agreement with values reported in the literature for heavier reaction systems at slightly higher beam energy [25]. The velocities of the three moving sources determined by the fit with Eq. (1) of the experimental data are about $v_{s1}=0.06c$, $0.13c$ and $0.19c$, with uncertainties of $\approx 15\%$. The slope parameters ($T \approx 5$ MeV) for projectile-like and target-like sources are comparable, simply reflecting the overall mass symmetry in the entrance channels of the three studied reactions. The value obtained by the fit for the velocity associated to the QT emission is higher compared to that expected for perfect binary kinematics ($\approx 0.04c$), and for the QT source slightly higher values for the slope parameters of ${}^7\text{Li}$ compared to ${}^7\text{Be}$ ones are also observed; these effects are probably due to the already mentioned identification thresholds that do not permit a good reconstruction of the QT emission. The slope parameters for the mid-velocity source are high ($T \approx 10$ MeV) for all the studied reactions.

${}^7\text{Li}$ and ${}^7\text{Be}$ production cross sections, $\sigma_i({}^7\text{Li})$ and $\sigma_i({}^7\text{Be})$, for the i^{th} source can be estimated by means of the expression $\sigma_i = 2N_i(\pi T_i)^{3/2}$, with N_i and T_i deduced from the best-fit analysis shown on Figure 3 [20,21]. Then, we calculate the isobaric ratios, $X_7 = \sigma_i({}^7\text{Li})/\sigma_i({}^7\text{Be})$, for each reaction and each source. Unfortunately, due to the identification thresholds, we observed that the X_7 values obtained for the QP and QT sources in ${}^{40}\text{Ca}+{}^{40}\text{Ca}$ reaction are different, and this is unphysical from symmetry arguments. In order to overcome this problem we can assume that the QT emission shows a systematic error introduced by the fitting procedure. We can reasonably assume as systematic error the difference $\varepsilon \equiv [X_7^{\text{QT}} - X_7^{\text{QP}}]_{40\text{Ca}+40\text{Ca}}$. In Figure 4 we show the X_7 obtained with the fit procedure, for all the reactions and all the emitting sources, where the QT emission has been corrected for the systematic error.

In Figure 4 we see a mid-velocity emission characterized by X_7 values higher than the QP emission ones, also for the isospin symmetric reaction ${}^{40}\text{Ca}+{}^{40}\text{Ca}$. This finding is in agreement with the results shown in paragraph 3, obtained looking at the parallel velocity spectra of light isotopes. Therefore, we observe that neutron rich isotopes and isobars are emitted with more probability in the mid-velocity part of the phase-space.

If we look at the isobaric emission for the QP source, we observe that even if the projectile used was the same for the three reactions (${}^{40}\text{Ca}$), the X_7 values increase with increasing N/Z content of the *target* nucleus. This effect, in agreement with the experimental findings of Section 3, testifies that, before the re-separation, isospin diffusion takes place between the projectile and target interacting nuclei. In particular, greater is the difference in N/Z between projectile and target nuclei, and greater is the net neutron diffusion along the whole di-nuclear system formed during the nuclear reaction.

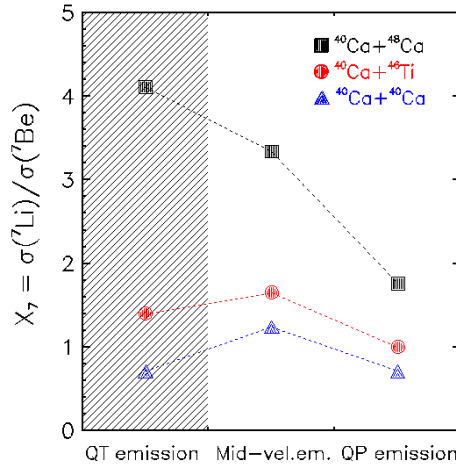


Fig. 4: Isobaric yield ratios ${}^7\text{Li}/{}^7\text{Be}$ for the three different reactions, as obtained from the moving source analysis. QP, QT and MV emissions are indicated. The X_7 values for QT emission have been corrected by the systematic error; for this reason the shadow area have to be regarded with some caution.

In order to understand if the isospin diffusion leads to the complete charge equilibration between the complementary QP and QT sources, we can look at the X_7 ratios for the QT emission. We can observe, for the strongly isospin asymmetric ${}^{40}\text{Ca}+{}^{48}\text{Ca}$ reaction, that the X_7 value associated to the QT source of emission is noticeably greater than the X_7 value related to the QP emission. This could be due to the fact that the relatively short interaction time does not allow a complete charge equilibration between the QP and QT sources; for this reason the X_7 value for the QT source still maintains a memory of the N/Z of the entrance target nucleus (${}^{48}\text{Ca}$), being higher than the corresponding X_7 value for the complementary QP emission. However we want to stress another time that, because of the high isotopic identification threshold given by the ΔE -E technique, QT emission is partially cut and it has to be regarded with some caution.

5 Conclusions and perspectives

Isospin diffusion, isospin drift and charge equilibration phenomena involving semi-peripheral nuclear reactions at 25MeV/A have been investigated looking at the emission of light isotopes (${}^6,{}^7\text{Li}$, ${}^7,{}^9\text{Be}$) and isobars (${}^7\text{Li}$ and ${}^7\text{Be}$) by means of the CHIMERA multi-detector. A neutron enrichment of the nuclear clusters emitted at mid-velocity is observed, in agreement with the isospin drift theory for nuclear reactions at intermediate energies. Isospin diffusion phenomena are observed, especially for the reaction ${}^{40}\text{Ca}+{}^{48}\text{Ca}$, having strong difference of N/Z between projectile and target. Looking at the isobaric yield ratios, obtained through a multi component moving source analysis of the kinetic energy spectra, it is possible to infer that the charge equilibrium through the di-nuclear systems is not reached before the re-separation of quasi-projectile and quasi-target sources. For the future we hope to perform the same collisions with more statistics; in this way we will disentangle the impact parameter dependence of isospin diffusion and charge equilibration related phenomena. Moreover with the recent tuning of the pulse shape technique for CHIMERA silicon detectors it will be possible to lower considerably the isotopic identification thresholds (until $\approx 3\text{MeV/A}$ for Li and Be isotopes); this improvement will allow a better reconstruction of the quasi-target emission.

References

- [1] D. A. Bromley, *Treatise on Heavy Ion Science*, Vol. 2, Chap. 3, Plenum Press NY (1984)
- [2] M. Di Toro *et al*, *Eur. Phys. Jour. A* **30** (2006) 65
- [3] M. Papa *et al*, *Phys. Rev. C* **75** (2007) 054616
- [4] E. De Filippo *et al*, *Phys. Rev. C* **71** (2005) 044602
- [5] E. Geraci *et al*, *Nucl. Phys. A* **734** (2004) 524
- [6] B.A. Li and W.U. Schröder, *Isospin Physics in Heavy Ion Collisions at Intermediate Energies*, Nova Science Publisher (2001)
- [7] F. Amorini *et al*, *Phys. Rev. Lett.* **102** (2009) 112701
- [8] B. Gatty *et al*, *Nucl. Phys. A* **253** (1975) 511
- [9] R. Planeta *et al*, *Phys. Rev. C* **38** (1988) 195
- [10] M. B. Tsang *et al*, *Phys. Rev. Lett.* **92** (2004) 062701
- [11] B.A. Li *et al*, *Phys. Rev. C* **71** (2005) 014608
- [12] M. Papa and G. Giuliani, *Eur. Phys. Jour. A* **39** (2009) 117
- [13] J. Łukasik *et al*, *Phys. Rev. C* **55** (1997) 1906
- [14] J. Töke *et al*, *Phys. Rev. Lett.* **75** (1995) 2920
- [15] E. Galichet *et al*, *Phys. Rev. C* **79** (2009) 064614
- [16] M. Veselsky *et al*, *Phys. Rev. C* **62** (2000) 041605(R)
- [17] M. B. Tsang *et al*, *Phys. Rev. Lett.* **102** (2009) 122701
- [18] F. Porto *et al*, *Acta Phys. Pol.* **31** (2000) 1489
- [19] A. Pagano *et al*, *Nucl. Phys. A* **734** (2004) 504
- [20] N. Le Neindre *et al*, *Nucl. Instrum. Meth. Phys. Res. A* **490** (2002) 251
- [21] J. Brzychczyk *et al*, *Phys. Rev. C* **47** (1993) 1553
- [22] E. De Filippo *et al*, *Acta Phys. Pol.* **37** (2006) 199
- [23] T. C. Awes *et al*, *Phys. Rev. C* **25** (1982) 2361
- [24] G. Lanzañò *et al*, *Phys. Rev. C* **58** (1998) 281
- [25] D. Santonocito *et al*, *Phys. Rev. C* **66** (2002) 044619
- [26] D. V. Shetty *et al*, *Phys. Rev. C* **68** (2003) 054605